

Acquisition and analysis of the optimal nutrient solution temperature range for lettuce using U-chord curvature

Huimin Li^{1,2}, Miao Lu^{1,2}, Kaikai Yuan^{1,2}, Mingke Zhang³, Dong Wang^{1,2}, Jin Hu^{2,4*}

(1. College of Mechanical and Electronic Engineering, Northwest A&F University, Yangling 712100, Shaanxi, China;

2. Key Laboratory of Agricultural Internet of Things, Ministry of Agriculture, Yangling 712100, Shaanxi, China;

3. College of Horticulture, Northwest A&F University, Yangling 712100, Shaanxi, China;

4. College of Information Engineering, Northwest A&F University, Yangling 712100, Shaanxi, China)

Abstract: Extreme nutrient solution temperature significantly affects photosynthetic characteristics of hydroponic vegetables and gives rise to slow plant growth. In this study, a method was proposed to obtain the suitable nutrient solution temperature range of hydroponic crops. Nested experiments of net photosynthetic rates were designed. The experiments considered the impact of nutrient solution temperatures, air temperatures, photon flux densities, and CO₂ concentrations. Then we established a prediction model of photosynthetic rate based on a regression support vector machine. The results have shown that the coefficient of determination between the measured values and the predicted values of photosynthetic rate is 0.982, and the root mean square error is 0.990 $\mu\text{mol}/\text{m}^2\cdot\text{s}$. Taking the net photosynthetic rate prediction model as the objective function, the maximum photosynthetic rate could be found using multiple population genetic algorithms, and then the nutrient solution temperature response curve could be created. According to the U-chord curvature theory, the suitable nutrient solution temperature range was calculated. After optimization by the multi-population genetic algorithm, the coefficient of determination between measured values and optimized values of maximum photosynthetic rate was 0.989 and the mean square error was 0.003. An analysis of the calculation based on the theory of U-chord curvature indicated that the suitable nutrient solution temperature range to grow hydroponic lettuce is 20.04°C–26.32°C. The proposed method provides a solid foundation to accurately acquire the suitable nutrient solution temperature range for a crop grown in hydroponics.

Keywords: photosynthetic rate, suitable nutrient solution temperature range, multiple population genetic optimization, U-chord curvature

DOI: 10.25165/j.ijabe.20241706.7729

Citation: Li H M, Lu M, Yuan K K, Zhang M K, Wang D, Hu J. Acquisition and analysis of the optimal nutrient solution temperature range for lettuce using U-chord curvature. *Int J Agric & Biol Eng*, 2024; 17(6): 93–100.

1 Introduction

As the main indicator for evaluating the accumulation of dry matter in plants, photosynthesis is mainly affected by environmental factors such as air temperature (AT), CO₂ concentration (CO₂), and photosynthetic photon flux density (PPFD)^[1-3]. In particular, nutrient solution temperature (TNS) directly affects root growth and nutrient absorption in hydroponically grown crops^[4,5]. During the growth of lettuce, the TNS is easily affected by high temperature in summer and low temperature in winter. It limits root growth and nutrient absorption and fails to satisfy the growth requirements of aboveground plant organs^[6,7]. Huang et al.^[8] believed that photosynthetic rate (Pn), root fresh weight, root number, N, P, and K contents of bentgrass decreased with the increase of TNS, thus

accelerating root mortality and affecting root growth rate and nutrient accumulation. Taranet et al.^[9] found that the increase of root zone temperature inhibited the accumulation of dry matter in sweet potato roots, and this effect increased with the increasing root zone temperature. When the temperature exceeded 40°C, the root tubers and the content of dry matter would decrease significantly. In addition, many studies have focused on the plant response to TNS from different perspectives, explored the physiological mechanisms by which plants are affected by TNS, and provided a theoretical basis for the regulation of TNS^[2,10]. Many experimental studies have shown that changes in leaf photosynthetic components, chlorophyll fluorescence parameters, and photosynthetic physiological parameters reflecting the intensity of photosynthesis can be significantly observed by controlling TNS^[2,5,10,11]. Therefore, it is critical to explore the effects of plant photosynthesis influenced by TNS and obtain the optimal TNS range for plants.

However, the photosynthesis of plants is usually not determined by changes in a single environmental factor alone, but rather by the combined effects of several environmental factors^[2-4]. To explore the synergistic regulatory effects of multiple environmental factors, we selected several environmental factors that have a significant impact on plant photosynthetic capacity based on previous research. AT is a critical factor affecting enzyme activity within the photosynthetic machinery and overall plant metabolism^[1,12]. Carbon dioxide is a fundamental substrate in the photosynthetic process. CO₂ affects multiple aspects including carbon fixation efficiency, photosynthetic rate, stomatal regulation,

Received date: 2022-06-08 **Accepted date:** 2024-07-02

Biographies: **Huimin Li**, MS candidate, research interest: agricultural information technology, Email: 2022051030@nwfufu.edu.cn; **Miao Lu**, PhD candidate, research interest: agricultural information technology, Email: lunalu0804@163.com; **Kaikai Yuan**, MS candidate, research interest: agricultural information technology, Email: a18309292816@163.com; **Mingke Zhang**, PhD, Professor, research interest: efficient cultivation and breeding of protected agricultural vegetables, Email: zhangmk0904@sina.com; **Dong Wang**, PhD, Associate Professor, research interest: Internet of Things technology in agriculture, Email: wangdong510@163.com.

***Corresponding author:** **Jin Hu**, PhD, Professor, research interest: agricultural sensors and information technology, College of Information Engineering, Northwest A&F University, Yangling 712100, Shaanxi, China, Tel: +86-13572502088, Email: jhudalab@163.com.

photosynthetic enzyme activity, and the accumulation of photosynthetic products^[2,13]. PPFd directly influences the photosynthetic rate by regulating the energy supply for photosynthesis. Appropriate PPFd levels can enhance photosynthetic efficiency, but excessive PPFd can limit the photosynthetic capacity of the plant^[3]. Therefore, synergizing the combined effects of multiple environmental factors is essential for building models of photosynthetic rate regulation.

Effective prediction and decision-making models play a crucial role in agricultural production and regulation. In recent years there have been many studies on prediction models of agricultural production due to the excellent nonlinear fitting capability and adaptability of machine learning algorithms such as neural network algorithms, support vector regression (SVR) algorithm, and so on. The neural network algorithms could capture complex nonlinear relationships in agricultural data^[13]. Li et al.^[14] established a photosynthetic rate prediction model based on back propagation (BP) neural network for quantitative regulation of CO₂ in greenhouses. Some studies have shown that the fuzzy neural network effectively handles uncertainty and variability in agricultural data, making it ideal for handling fluctuating environmental conditions^[15,16]. Zhang et al.^[17] built a tomato price time series prediction model using the wavelet neural network, which could effectively capture short-term and long-term environmental variations through wavelet transform feature extraction. However, neural network algorithms have problems such as complex parameter settings and susceptibility to overfitting^[18]. Currently, due to the advantages of SVR algorithm, such as simple parameter settings and strong fitting ability to high-dimensional data and nonlinear relationships, the research in agricultural applications is gradually increasing and showing significant results. Wei et al.^[19] built a photosynthetic rate prediction model using the SVR algorithm for the prediction of the cucumber photosynthetic rate during the whole growth period. Therefore, efficient algorithms need to be selected for modeling optimization to provide the technical basis for obtaining the optimal TNS range.

Traditional agricultural regulation often focuses on optimizing specific points. However, with the increasing complexity of agricultural production, single-point optimization may not adequately account for interactions and changes among multiple factors. Therefore, in practical applications, shifting to an interval optimization strategy appears more suitable and effective. This strategy comprehensively considers variations of different factors within specified ranges, rather than narrowly focusing on precise single-point adjustments. Interval optimization enables agricultural production to better adapt to environmental changes and seasonal variability, thereby enhancing production stability and efficiency. Curvature, as a morphological tool, plays a crucial role in analyzing and identifying local shape features within these intervals. Curvature is used to measure the degree of the curve unflatness and is often used for the acquisition of curve feature points. An explicit functional relationship of the curve is required to traditionally calculate the curvature value. Therefore, Guo and Zhong^[20] proposed the U-chord curvature, which can calculate the curvature values of discrete points and has good robustness. In the agricultural field, Gao et al.^[21] proposed a method based on U-chord curvature to avoid excessive consumption of light and CO₂ resources and improve the photosynthetic rate. Hu et al.^[22] obtained the optimal soil moisture content regulation range under photosynthetic rate constraints by applying the U-chord curvature to the response discrete curves of photosynthetic rate to the soil moisture content.

These studies demonstrated the rationality of using U-chord curvature to obtain the optimal TNS range.

This study explored the photosynthetic characteristic of hydroponic lettuce under different TNS, AT, CO₂, and PPFd. The Pn prediction model was established by using support vector machine regression (SVR) algorithm. A multi-population genetic algorithm (MPGA) was used to obtain the optimum AT, CO₂, PPFd, and the corresponding maximum Pn (MPn) under different TNS. Then, the response curve of MPn to TNS was obtained. The optimal TNS range was calculated based on U-chord curvature theory. The acquisition of optimal TNS range provides a theoretical foundation for the growth of protected crops.

2 Materials and methods

2.1 Experimental materials and data acquisition

2.1.1 Experimental materials

The experiment was conducted in the College of Mechanical and Electronic Engineering, Northwest Agriculture and Forestry University (at 34°07'39''N, 107°59'50''E, and 648 m above sea level). The researched samples of cream lettuce were acquired from the Modern Agricultural Demonstration and Innovation Park in Yangling District, Xianyang City, Shaanxi Province. The experiment was carried out using hydroponics^[23]. The hydroponic cultivation box was 40 cm×20 cm×15 cm, with a capacity of 8 L. The hydroponic nutrient solution was prepared as listed in Table 1. Healthy seedlings with 4 to 5 leaves and a leaf size reaching 3×5 cm were selected for the experiment. On the first day of the experiment, the lettuce seedlings were transferred to MD1400 incubator (Snijders, the Netherlands) to pre-adapt the seedlings to the environment. The incubator is shown in Figure 1. The incubator was set to conditions at a temperature of 25°C, humidity of 50%, and CO₂ of 400 μL/L. To effectively avoid the “midday break” phenomenon, the test was performed from 8:30-11:30 and from 14:30-17:30. No pesticides were sprayed during the experiment, following the normal management of the greenhouse hydroponic system.

Table 1 Prescription of the hydroponic nutrient solution

Ingredient	Content /mmol·L ⁻¹
Ca(NO ₃) ₂ ·5H ₂ O	5
(NH ₄) ₂ SO ₄	5
K ₂ SO ₄	0.75
KH ₂ PO ₄	0.5
KCl	0.1
MgSO ₄ ·7H ₂ O	0.65
H ₃ BO ₃	1.0×10 ⁻³
MnSO ₄ ·H ₂ O	1.0×10 ⁻³
CuSO ₄ ·5H ₂ O	1.0×10 ⁻⁴
ZnSO ₄ ·7H ₂ O,	1.0×10 ⁻³
(NH ₄) ₆ Mo ₇ O ₂₄ ·4H ₂ O	5×10 ⁻⁶
EDTA-Fe	0.1

2.1.2 Data acquisition

The photosynthetic rate was measured by using Li-6800XT portable photosynthesis instrument (LI-COR, USA). During the experiment, multiple sub-modules selected by the photosynthesis instrument were used to control the temperature, CO₂, and PPFd around the leaf as required. Temperature control block set 5 AT gradients (10°C, 15°C, 20°C, 25°C, and 30°C). CO₂ injection block set 3 CO₂ volume ratio gradients (400, 800, and 1200 μL/L). LED light source block set 9 PPFd gradients (0, 20, 50, 100, 300, 500,

550, 600, and 700 $\mu\text{mol}/\text{m}^2\cdot\text{s}$). The humidification block set the chamber humidity to 50%. In addition, water temperature heating block set 9 TNS gradients (13°C, 15°C, 17°C, 19°C, 21°C, 23°C, 25°C, 27°C, and 29°C). A total of 810 nested experiments were

performed. Three plants of the same age were randomly selected from each group as replicates to form a set of 810 groups of experimental samples with AT, CO₂, PPFD, and TNS as inputs, and the Pn as output. The experimental equipment is shown in Figure 1.

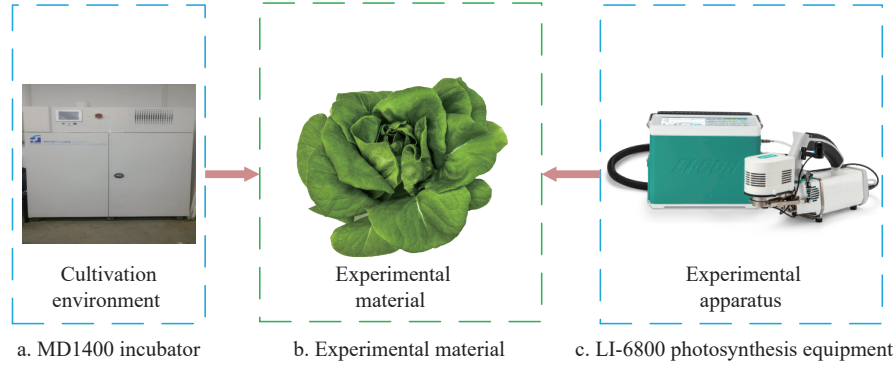


Figure 1 Experimental equipment

2.2 Data pre-processing

Considering the inconsistent dimensionality of the four-dimensional data, the data of different dimensions, such as TNS, AT, CO₂, and PPFD, were normalized. The range of normalization was $[-1, 1]$. The 810 sets of sample data were randomly divided into training and test sets in a ratio of 8:2. 650 groups of sample datasets were randomly selected as the training set. 160 groups of sample datasets were randomly selected as the validation set. The training set and test set sample were used for the construction and training of the Pn prediction model, respectively.

2.3 Modeling and determination of targets

This study constructed the Pn prediction model by SVR algorithm. The corresponding response curves of maximum photosynthetic rates under different TNS conditions were obtained by applying the optimization algorithm of MPG. The curvature curve was calculated based on U-chord curvature theory. In addition, the local maximum value point of the curvature was obtained by the mountain climbing method and defined as the curvature feature points, which were used as regulation targets. The optimization process of the TNS response curve is shown in Figure 2.

2.3.1 Prediction model of photosynthetic rate

Considering the advantages of the SVR algorithm, such as its robustness to overfitting and effective handling of high-dimensional data, this study used the SVR algorithm to construct a photosynthetic rate prediction model.

TNS, AT, CO₂, and PPFD were used as inputs of the Pn prediction model, and the Pn was used as output of the model. The input signals were defined as $X = (x_1, x_2, x_3, x_4)$, where $x_1, x_2, x_3,$ and x_4 were TNS, AT, CO₂, and PPFD, respectively. The Pn prediction model $f(x)$ was established by using SVM algorithm. The decision function is shown in Equation (1).

$$f(x) = w\Phi(x) + b = \sum_{i=1}^l (a_i - a_i^*)K(x_i, x) + b \quad (1)$$

where, $K(x_i, x_j) = \Phi(x_i)\Phi(x_j)$ is the kernel function; \bar{a}_i^* , \bar{a}_i is the Lagrange multiplier; l is the number of support vectors; w is the weight vector; and b is the offset.

The selection of an appropriate kernel function and parameters c and g was essential to construct the model and find optimization. The complexity of the radial basis function was invariant with the change of parameters in the calculation process by comparing the

radial basis function, the linear function, and the polynomial function. Thus, the radial basis function was selected to construct the prediction model as shown in Equation (2).

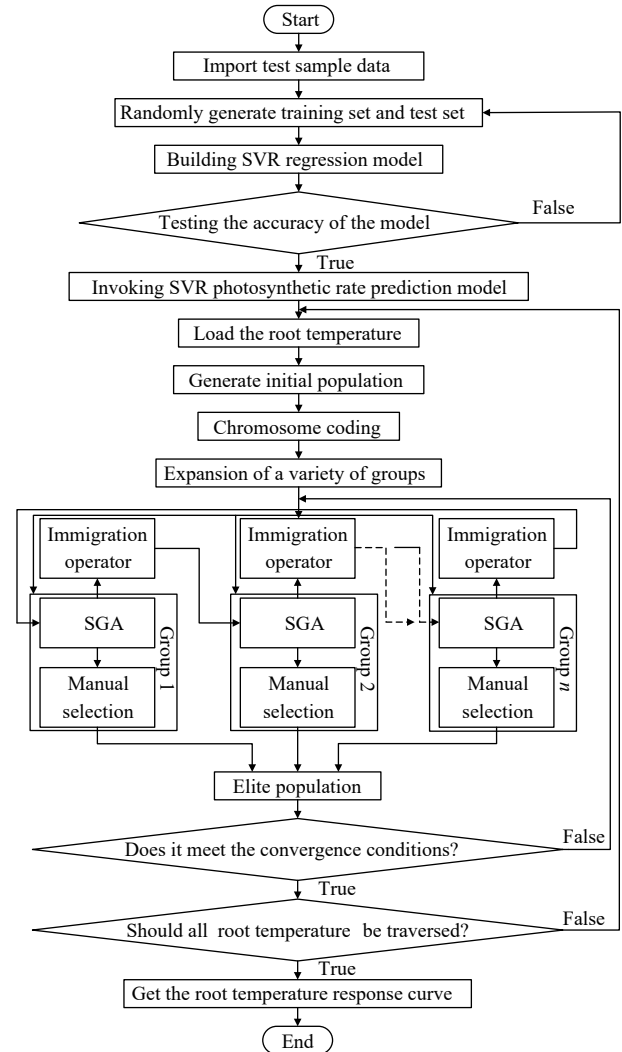


Figure 2 TNS response curve optimization flow chart

$$K(x, x_i) = \exp(-\sigma \times \|x_i - x\|^2) \quad (2)$$

where, σ is width information; x is input signal; and x_i is input of the training sample.

After cross-validation, the parameters under different combinations were calculated several times. Finally, the optimal parameter value for c was 5.657 and for g was 0.250.

Meanwhile, we also employed the commonly used BP neural network (BP), wavelet neural network, and fuzzy neural network algorithms to construct a photosynthetic rate prediction model for comparison in order to validate the modeling effectiveness of the SVR model. The BP network is trained using the backpropagation algorithm and can adapt to complex nonlinear relationships; the wavelet neural network utilizes wavelet transform for feature extraction and has advantages in handling time series data and frequency domain data; while the fuzzy neural network, by introducing fuzzy logic to handle the uncertainty and fuzziness of the data, is suitable for dealing with the variability of environmental conditions. These algorithms were implemented in Python.

2.3.2 MPn discrete curves acquisition

In the standard genetic algorithm (SGA), the selection of the values of P_c and P_m is random. For different options, the optimization results vary greatly^[24-26]. The multi-population genetic algorithm compensates for the deficiency of the SGA and evolves through multiple populations with different control parameters. Due to the algorithm's concurrent global search and local search ability, the optimization results of the algorithm are more accurate^[27-29]. Therefore, on the basis of the Pn prediction model, the multi-population genetic algorithm (MPGA) was used to find the optimal AT, CO₂, PPF, and the corresponding MPn under different TNS. Then, the MPn curve under different TNS was obtained.

First, the individual length of the initial population was 40. TNS was used as a variable, and AT, CO₂, and PPF as the optimization objective to find the MPn. The initial population $P(t)$ was generated randomly and divided according to the information exchange model: $P(t) = \{P_1(t), \dots, P_i(t), \dots, P_n(t)\}$, in which n was the number of groups. Then the individual's fitness $P_i(t)$, ($i = 1, 2, \dots, n$) was calculated by grouping.

Second, the values of P_c and P_m determined the balance between the algorithm's global search and the local search ability. They can be calculated according to Equation (3):

$$\begin{cases} P_c(G) = P_c(1) + cf_{rand}(M, 1) \\ P_m(G) = P_m(1) + mf_{rand}(M, 1) \end{cases} \quad (3)$$

where, $P_c(1)$ is the initial crossover probability and $P_m(1)$ is the mutation probability; G is the genetic manipulation algebras; c , m are interval lengths of the crossover and mutation operations, respectively; M is the population numbers; and f_{rand} is the function that generated random numbers.

Finally, multi-population co-evolution can be realized by connecting with the immigration factor. The worst individual in the target population was replaced by the optimal individual from the source population. The best individual from the other populations was manually selected and was put into the elite population for preservation in every generation of the evolution process. Genetic manipulations, such as selection, crossover, and mutation, were not performed for elite populations to ensure that the optimal individuals produced by various groups were not destroyed or lost.

The optimal temperature, CO₂, PPF, and the corresponding MPn under different TNS conditions were obtained. Then, the MPn discrete curves were obtained.

2.3.3 Discrete curvature of the MPn-TNS response curve

The U-chord curvature method was adopted to calculate the discrete curvature of the TNS response curve. The solution process

is as follows:

First, the parameters U and current point $P_i(x,y)$ were determined, starting with the current point to move back and front. The discrete points with Euclidean distances larger than the values of U were used as the initial support of the current field. Discrete digital curves could satisfy the constraint conditions approximately. Therefore, the implicit strategy was used to enhance the accuracy of the calculation. Eventually, the support domain $[P_i^b, P_i^f]$ was obtained by refining the digital curve. Figure 3 describes the method for determining the support domain of U-chord curvature.

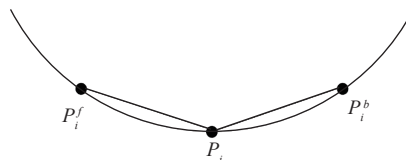


Figure 3 P_i support neighborhood

In the final support domain, a cosine value related to the included angle of the front and rear arm vectors in the support domain was used as the discrete curvature. The specific calculation equation is shown as follows:

$$c_i = s_i \sqrt{1 - \left(\frac{D_i}{2U}\right)^2} \quad (4)$$

where, $s_i = \text{sign}[(x_i - x_i^b)(y_i^f - y_i^b) - (x_i^f - x_i^b)(y_i - y_i^b)]$

P_i is the data point on the response curve of screened chlorophyll fluorescence parameters to nitrogen concentration; $[P_i^b, P_i^f]$ is the support area for P_i points; D_i is the distance between two points P_i^b and P_i^f ; S_i is the symbol of discrete curvature values; (x_i^b, y_i^b) are the coordinates of P_i^b ; (x_i^f, y_i^f) are the coordinates of P_i^f ; and (x_i, y_i) are the coordinates of P_i .

2.3.4 The feature point of the curvature response curves

Based on the curvature response curve, the local maximum value point of the curvature was obtained by the mountain climbing method. In discrete curve of MPn response, the local maximum value point was the feature point of its response curve. The Pn among the curvature feature points was high and the lettuce grew well. The method of mountain climbing is to continuously detour, evaluate the difference between two adjacent points, determine the direction of progress, and continue to detour until reaching the top of the mountain. The steps are as follows:

- 1) The initial point q_k and the initial direction are selected. Then, the algorithm runs in the initial direction.
- 2) The curvature c_{k-1} and c_{k+1} at the two adjacent points q_{k-1} and q_{k+1} are compared. If $c_{k-1} < c_k < c_{k+1}$, it has not reached the top of the mountain and continues to move in the positive direction. If $c_{k-1} > c_k > c_{k+1}$, it changes the forward direction and continues in the opposite direction.
- 3) The status is tested by repeating Step 2 until the point reaches $c_{k-1} < c_k > c_{k+1}$. Then, the test is stopped and the result is returned.
- 4) If no peak is found at the end of the test, it goes back and continues the test in the opposite direction from the initial state.

The two local maximum points adjacent to the global maximum point on U-chord curvature response curve and the corresponding TNS were recorded. The temperature range between the two TNS values is the optimal TNS range for lettuce growth.

2.4 Evaluation of predictive model performance

During the modeling process, the performance of the Pn prediction model was verified by applying different check methods,

such as the root mean square error (RMSE), average absolute error (AAE), average relative error (ARE), and determination factor (R^2).

$$\text{RMSE} = \sqrt{\frac{\sum_{i=1}^N (f(X_i) - Y_i)^2}{N}} \quad (5)$$

$$\text{AAE} = \frac{1}{N} \sum_{i=1}^N |f(X_i) - Y_i| \quad (6)$$

$$\text{ARE} = \frac{1}{N} \sum_{i=1}^N (|f(X_i) - Y_i| / Y_i) \quad (7)$$

$$R^2 = 1 - \frac{\sum_{i=1}^N (f(X_i) - Y_i)^2}{\sum_{i=1}^N \left(Y_i - \frac{1}{N} \sum_{i=1}^N Y_i \right)^2} \quad (8)$$

,where $f(X)$ denotes the predicted value of the photosynthetic rate model corresponding to the input feature X ; N denotes the number of samples; and Y_i represents the measured Pn data of the i^{th} sample.

3 Results

3.1 Comparison of modeling methods for Pn prediction models

The method considered and selected several environmental factors (TNS, AT, CO_2 , and PPF) as inputs, and net photosynthetic rate as output) in order to establish the Pn prediction model. However, the multidimensional input in the modeling process increased the complexity of the model, which reduced the accuracy. Therefore, it was particularly important to select an appropriate modeling method. This paper selected modeling methods such as BP neural network (BP), wavelet neural network, fuzzy neural network, and regression support vector machine (SVR) to build the model. The optimal modeling method was selected by the root mean square error, average absolute error, average relative error, determination coefficient R^2 , and other indicators. The results indicated that the Pn prediction model established by SVR algorithm was accurate. The specific results are listed in Table 2.

Table 2 Comparison of evaluation indices from different modeling methods

Forecast model	Root mean square error	Average absolute error/%	Average relative error/%	R^2
BP	1.314	0.379	9.141	0.974
Wavelet neural network	3.782	8.374	13.125	0.933
Fuzzy neural network	2.825	0.205	14.098	0.948
SVR	0.990	2.667	2.950	0.982

Based on the above comparison and analysis of modeling methods, the optimal modeling method was obtained, and the photosynthetic rate prediction model was established. The error for each model between the measured values and the predicted values of Pn were used as the benchmarks for model validation. Based on 160 sample data from the validation set, the comparison of the measured and the predicted value of the Pn is shown in Figure 4. The model determination coefficient is 0.982. The slope of the linear line is 0.9424, and the intercept of the vertical axis is 0.6225, which suggests a good fitting degree.

3.2 Optimization algorithm comparison analysis

The optimal AT, CO_2 , PPF, and corresponding MPn under

different TNS were obtained by the TNS response curve. Therefore, standard genetic algorithms and multi-population genetic algorithms were respectively used to perform optimizations. In order to effectively avoid the occurrence of accidental events, TNS of 17°C as an example, random optimization was performed five times. The available evolution process is shown in Figure 5.

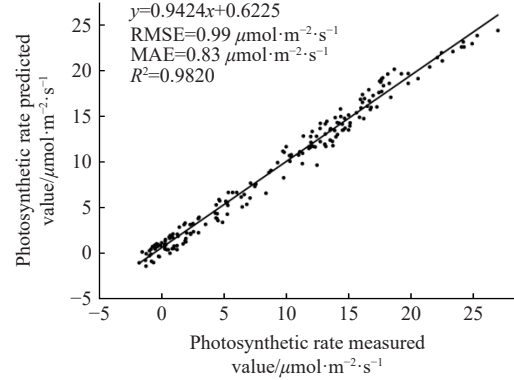
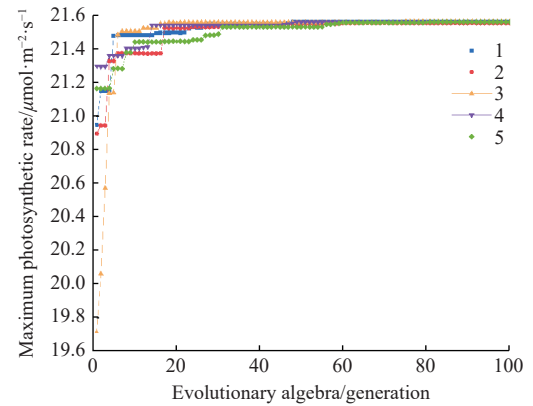
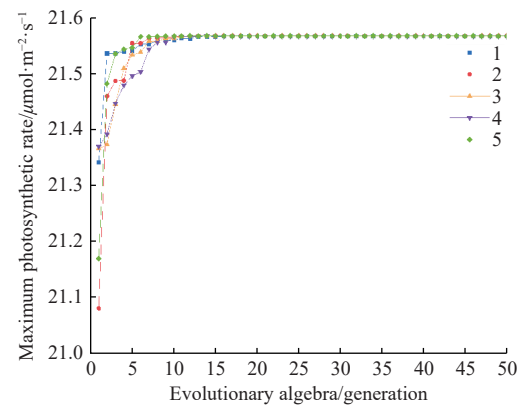


Figure 4 Verification of the Pn prediction model



a. The evolutionary process map of SGA optimization



b. The evolutionary process map of MPGA optimization

Figure 5 Optimization evolutionary process

As shown in Figure 5a, when the standard genetic algorithm evolved at least 100 generations, the AT, CO_2 , and PPF under different TNS tended to be stable. As shown in Figure 5b, when the multi-population genetic algorithm evolved up to 14 generations, the AT, CO_2 , and PPF under different TNS tended to be stable without oscillation or partial flat area in the training process.

As shown in Table 3, maximum error analyses were performed five times for the results of random optimization. The results from MPGA showed that the optimal PPF and the MPn error for the

random optimization of five populations were zero. The maximum errors of the optimum PPFD and optimum CO₂ obtained by the random optimization of SGA were 0.377 and 15.971, respectively. Therefore, MPGA had higher search precision and stability than SGA.

Table 3 Analysis of the maximum error of standard genetic and multi-population genetic optimization

Optimization algorithm optimum	Error of optimum AT/°C	Error of optimum PPFD/($\mu\text{mol}\cdot\text{m}^{-2}\cdot\text{s}^{-1}$)	Error of optimum CO ₂ /($\mu\text{L}\cdot\text{L}^{-1}$)	Error of MPn/($\mu\text{mol}\cdot\text{m}^{-2}\cdot\text{s}^{-1}$)
SGA	0.317	0.377	15.971	0.004
MPGA	0	0	0.002	0

Based on the analysis of the above optimization results, in order to further verify the optimization accuracy of MPGA, the algorithm was repeated to obtain maximum photosynthetic values at different TNS (13°C, 15°C, 17°C, 19°C, 21°C, 23°C, 25°C, 27°C, and 29°C). Then, the predicted values of Pn were compared with the corresponding measured values of Pn, the determination coefficient was 0.989, and the root mean square error was 0.003. The experiment not only verified the accuracy and reliability of the Pn prediction model, but also verified the accuracy of the optimization result of MPGA, which could provide theoretical support for obtaining the optimal TNS range.

The optimal values of AT, PPFD, CO₂, and corresponding MPn under different TNS were obtained based on MPGA Pn prediction model. The MPn response curves under different TNS were obtained as shown in Figure 6.

3.3 Suitable TNS range

The curvature of the MPn-TNS response curve was calculated by curvature theory. The TNS values corresponding to the curvature feature points were 20.04°C, 23.23°C, and 26.32°C, respectively. According to the response curve of Pn to TNS, the MPn was in the optimum range when TNS was in the range of 20.04°C to 26.32°C (Figure 7), and it reached the optimal level when the temperature

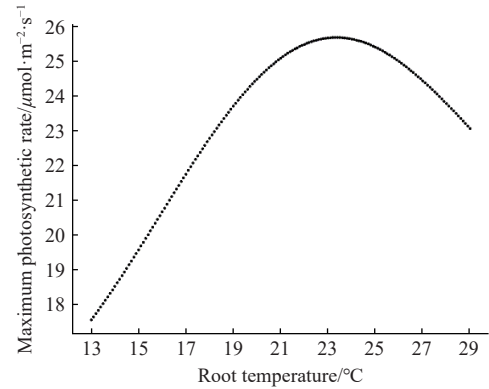


Figure 6 MPn curve at different TNS

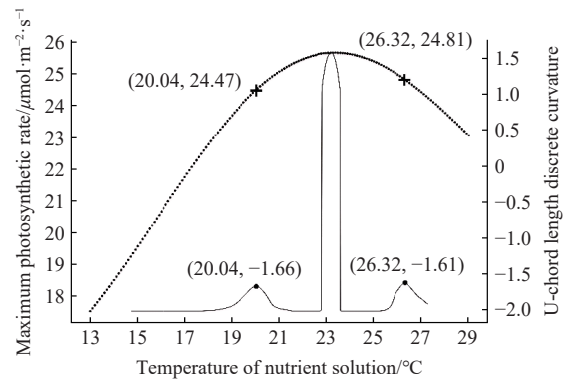


Figure 7 U-chord curvature response curve and feature point

was 23.23°C. Therefore, the suitable TNS range of lettuce growth is 20.04°C-26.32°C. In the suitable range of TNS, the Pn is high in different environments (Figure 8).

In order to further verify the cultivation effect of the suitable TNS range, the hydroponic lettuces from two areas of 5 m× 4 m were selected to take a test and carry out a 30-d natural control treatment. The lettuce cultivar was still “cream lettuce”. Among them, the TNS control device was used to keep the TNS in the

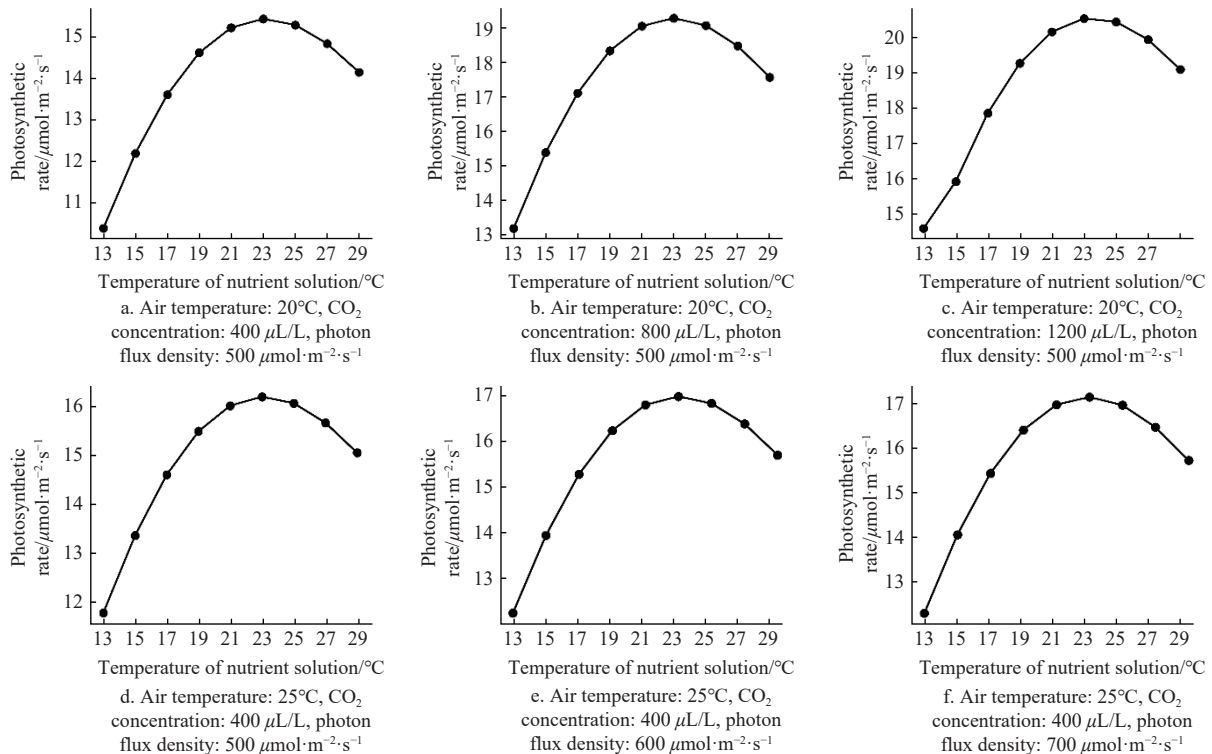


Figure 8 Example verification of light response curves in different circumstances

suitable range. The natural control treatment used a conventional culture mode without any intervention. These two treatment zones were subjected to standard hydroponic management during the test. The treatments were carried out at the seedling stage. 15 samples were randomly selected from the two treatment zones for weighing when these samples were cultured to 30 days. The average weight of the samples cultured in the test treatment area was 335 g. The average weight of the samples cultured in the natural control area was 280 g. The results suggested that the average weight of the samples cultured in the test treatment area increased by 19.6% compared with the natural control area. Therefore, the suitable TNS range has a good promotion effect on the growth of hydroponic crops.

4 Discussion

Building a stable and accurate photosynthetic rate prediction model is the foundation for TNS optimization. The SVR algorithm and three neural network algorithms were used to build photosynthetic rate prediction models for comparison. As shown in Table 1, the SVR model had the highest R^2 and the lowest RMSE, indicating that the difference between its predicted and actual values was the smallest and the model had the highest prediction accuracy. In terms of AAE value, BP and fuzzy neural network had low values, indicating that they perform well in terms of absolute error. This implies that the models obtained from the BP and fuzzy neural network algorithms have less average deviation between predicted and true values and are more suitable for situations where the data magnitude is consistent. However, SVR performed significantly better than the other models in ARE value, which suggests that it is more stable when dealing with different orders of magnitude of data. Many studies have shown that BP neural networks are prone to an overfitting phenomenon in the training process, the parameter settings are complicated, and the training time is long^[30]. On the other hand, wavelet neural network and fuzzy neural network have the problems of high model complexity and large computational cost^[31,32]. However, the superior performance of SVR algorithm is mainly attributed to its ability to handle high-dimensional feature space and good generalization ability. In addition, the SVR algorithm can effectively deal with nonlinear data and improve the robustness and stability of the model through appropriate kernel function selection. Given the actual modeling needs of photosynthetic rate prediction models and the performance of these four algorithms, we concluded that the SVR algorithm not only has the advantages of high model fit and high prediction accuracy, but also shows good stability and consistency under different data magnitudes.

The TNS of hydroponic crops directly affects root nutrient absorption, which causes a change in the photosynthetic characteristics of aboveground organs^[33,34]. The increased transpiration rate is due to increased TNS and increased root flow. It provides the PSII reaction center with a suitable environment, which contributes to photochemical reactions and electron transfer^[35]. The Pn greatly increases under suitable conditions. When TNS and AT increase to a certain extent, the transpiration rate gradually decreases and stomata on the leaf surface close. Under these conditions, the Pn gradually stagnates as the crop cannot perform adequate photosynthesis. Photosynthesis was in the optimal state when the TNS rose to 23.3°C. This is consistent with the law shown in the MPn response curve under different TNS (Figure 8). Furthermore, suitable TNS is beneficial to alleviate the cold stress in the aboveground organs, promote cell division and leaf area

expansion, and provide necessary conditions for the production of chlorophyll^[6,11]. Therefore, based on the response of the hydroponic crops to the TNS, the optimal TNS range for hydroponic crops is obtained by optimum Pn. This is important for improving crop yield and quality.

Based on the TNS response curve as shown in Figure 7, it is obvious that the curvature response curve shows multiple peaks, revealing the existence of curvature inflection points difficult to observe. Therefore, the curvature of TNS response curve was calculated to reflect the locations of all inflection points, which laid a foundation for the accurate acquisition of the optimal TNS range. This method not only ensures effective nutrient solution temperature regulation but also underscores the importance of precise environmental control in hydroponic cultivation, offering a solid theoretical basis for the environmental regulation of lettuce in other growth periods or other vegetables. In future work, we will expand the experimental data and incorporate additional physiological indicators (like leaf chlorophyll content, leaf weight, and other factors reflecting both immediate and long-term plant responses) to track physiological indicators over multiple growing seasons and explore deep insights about the sustained impacts of environmental factors on crop productivity.

5 Conclusions

This study proposed a method to optimize TNS regulation range for hydroponic crops by integrating external environmental factors into a Pn prediction model. The Pn prediction model was built by SVR with AT, CO₂, PPF, and TNS as inputs, which had high accuracy and great stability. Subsequently, a novel multi-population genetic algorithm was employed to obtain the maximum Pn curve with a determination factor of 0.989. The optimal TNS range obtained by the U-chord curvature and the climb method was 20.04°C-26.32°C. The validation experiment showed that within this temperature range, the average weight of hydroponic lettuce increased by 19.6% compared to the natural control group. The results indicate that the optimal TNS range identified in this study could address the needs of hydroponic crops. The proposed method in this research provides a theoretical foundation and offers new ideas for the precise regulation of nutrient solution temperature.

Acknowledgements

This work was supported by the National Key Research and Development Program of China (Grant No. 2020YFD1100602); the Shaanxi Key Research and Development Program (Grant No. 2023-ZDLNY-66); and the Shaanxi Provincial Science and Technology Program (Grant No. Z2024-ZYFS-0043). The authors appreciate the funding organizations for their financial support.

[References]

- [1] Shah N H, Paulsen G M. Interaction of drought and high temperature on photosynthesis and grain-filling of wheat. *Plant and Soil*, 2003; 257: 219–226.
- [2] Li D, Dong J, Gruda N S, Li X, Duan Z. Elevated root-zone temperature promotes the growth and alleviates the photosynthetic acclimation of cucumber plants exposed to elevated [CO₂]. *Environmental and Experimental Botany*, 2022; 194: 104694.
- [3] Gao P, Tian Z, Lu Y, Lu M, Zhang H, Wu H, Hu J. A decision-making model for light environment control of tomato seedlings aiming at the knee point of light-response curves. *Computers and Electronics in Agriculture*, 2022; 198: 107103.
- [4] He J, Tan L P, Lee S K. Root-zone temperature effects on photosynthesis, 14 C-photoassimilate partitioning and growth of temperate lettuce (*Lactuca*

- sativa* cv. 'Panama') in the tropics. *Photosynthetica*, 2009; 47: 95–103.
- [5] Xia Z, Zhang S, Wang Q, Zhang G, Fu Y, Lu H. Effects of root zone warming on maize seedling growth and photosynthetic characteristics under different phosphorus levels. *Frontiers in Plant Science*, 2021; 12: 746152.
- [6] Sakamoto M, Suzuki T. Effect of root-zone temperature on growth and quality of hydroponically grown red leaf lettuce (*Lactuca sativa* L. cv. Red Wave). *American Journal of Plant Sciences*, 2015; 6(14): 2350.
- [7] Sakamoto M, Uenishi M, Miyamoto K, Suzuki T. Effect of root-zone temperature on the growth and fruit quality of hydroponically grown strawberry plants. *Journal of Agricultural Science*, 2016; 8(5): 122–131.
- [8] Huang B, Xu Q. Root growth and nutrient element status of creeping bentgrass cultivars differing in heat tolerance as influenced by supraoptimal shoot and root temperatures. *Journal of Plant Nutrition*, 2000; 23(7): 979–990.
- [9] Taranet P, Kirchof G, Fujinuma R, Menzies N. Root zone temperature alters storage root formation and growth of sweetpotato. *Journal of Agronomy and Crop Science*, 2018; 204(3): 313–324.
- [10] Xia Z Q, Si L Y, Jin Y, Fu Y F, Wang Q, Lu H D. Effects of root zone temperature increase on physiological indexes and photosynthesis of different genotype maize seedlings. *Russian Journal of Plant Physiology*, 2021; 68: 169–178.
- [11] Kawasaki Y, Matsuo S, Suzuki K, Kanayama Y, Kanahama K. Root-zone cooling at high air temperatures enhances physiological activities and internal structures of roots in young tomato plants. *Journal of the Japanese Society for Horticultural Science*, 2013; 82(4): 322–327.
- [12] Yamori N, Levine C P, Mattson N S, Yamori W. Optimum root zone temperature of photosynthesis and plant growth depends on air temperature in lettuce plants. *Plant Molecular Biology*, 2022; 110(4): 385–395.
- [13] Dong Y, Fu Z, Peng Y, Zheng Y, Yan H, Li X. Precision fertilization method of field crops based on the Wavelet-BP neural network in China. *Journal of Cleaner Production*, 2020; 246: 118735.
- [14] Ting L, Man Z, Yuhan J, Sha S, Jiang Y Q, Li M Z. Management of CO₂ in a tomato greenhouse using WSN and BPNN techniques. *Int J Agric & Biol Eng*, 2015; 8(4): 43–51.
- [15] Liu S, Zhang W. Application of the fuzzy neural network algorithm in the exploration of the agricultural products E-commerce path. *Intelligent Automation & Soft Computing*, 2020; 26(3): 569–575.
- [16] Murmu S, Biswas S. Application of fuzzy logic and neural network in crop classification: a review. *Aquatic Procedia*, 2015; 4: 1203–1210.
- [17] Zhang J H, Kong F T, Wu J Z, Zhu M S, Xu K, Liu J J. Tomato prices time series prediction model based on wavelet neural network. *Applied Mechanics and Materials*, 2014; 644: 2636–2640.
- [18] Liu Y, Starzyk J A, Zhu Z. Optimized approximation algorithm in neural networks without overfitting. *IEEE Transactions on Neural Networks*, 2008; 19(6): 983–995.
- [19] Wei Z, Wan X, Lei W, Yuan K, Lu M, Li B, Gao P, Wu H R, Hu J. A cucumber photosynthetic rate prediction model in whole growth period with time parameters. *Agriculture*, 2023; 13(1): 204.
- [20] Guo J J, Zhong B J. U-chord curvature: a computational method of discrete curvature. *Pattern Recognition and Artificial Intelligence*, 2014; 27(8): 683–691.
- [21] Gao P, Li B, Bai J, Lu M, Feng P, Wu H, Hu J. Method for optimizing controlled conditions of plant growth using U-chord curvature. *Computers and Electronics in Agriculture*, 2021; 185: 106141.
- [22] Hu J, Long X X, Deng Y F, Wan X B, Li B, Wu H R. Water demand model for greenhouse crops considering water use efficiency and photosynthetic rate. *Transactions of the CSAM*, 2020; 51(10): 362–370. (in Chinese).
- [23] Chen D, Zhang J, Zhang Z, Lu Y, Zhang H, Hu J. A high efficiency CO₂ concentration interval optimization method for lettuce growth. *Science of The Total Environment*, 2023; 879: 162731.
- [24] Rajarathinam K, Gomm J B, Yu D L, Abdelhadi A S. An improved search space resizing method for model identification by standard genetic algorithm. *Systems Science and Control Engineering*, 2017; 5(1): 117–128.
- [25] Rajarathinam K, Gomm J B, Yu D L, Abdelhadi A S. Model parameters identification for excess oxygen by standard genetic algorithm. 22nd International Conference on Automation and Computing (ICAC), IEEE, 2016; pp.198–203.
- [26] Rajan N A, Shrikant K D, Dhanalakshmi B, Rajasekar N. Solar P V array reconfiguration using the concept of Standard deviation and Genetic Algorithm. *Energy Procedia*, 2017; 117: 1062–1069.
- [27] Cochran J K, Hornig S M, Fowler J W. A multi-population genetic algorithm to solve multi-objective scheduling problems for parallel machines. *Computers & Operations Research*, 2003; 30(7): 1087–1102.
- [28] Lu Z Y, Wang D M, Wang J H, Wang Y. Fusion location based on parallel genetic algorithm of multi-population. *Journal of Terahertz Science and Electronic Information Technology*, 2016; 14(2): 195–200.
- [29] Godio A. Multi population genetic algorithm to estimate snow properties from GPR data. *Journal of Applied Geophysics*, 2016; 131: 133–144.
- [30] Sarle W S. Stopped training and other remedies for overfitting. *Proceedings of symposium on the Interface of Computing Science & Statistics*, 1996; pp.352–360.
- [31] Zhang Q, Benveniste A. Wavelet networks. *IEEE Transactions on Neural Networks*, 1992; 3(6): 889–898.
- [32] Jang J S R, Sun C T, Mizutani E. Neuro-fuzzy and soft computing—a computational approach to learning and machine intelligence. *IEEE Transactions on Automatic Control*, 1997; 42(10): 1482–1484.
- [33] Xia Z, Zhang G, Zhang S, Wang Q, Fu Y, Lu H. Efficacy of root zone temperature increase in root and shoot development and hormone changes in different maize genotypes. *Agriculture*, 2021; 11(6): 477.
- [34] He J, Lee S K, Dodd I C. Limitations to photosynthesis of lettuce grown under tropical conditions: alleviation by root - zone cooling. *Journal of Experimental Botany*, 2001; 52(359): 1323–1330.
- [35] Wang B, Jeffers S N. Effects of cultural practices and temperature on Fusarium root and crown rot of container-grown hostas. *Plant Disease*, 2002; 86(3): 225–231.